Can Mechanical Stress Therapies be used in COVID-19 outbreak?

Muhammad Ali (m.alinaeem23@gmail.com)
Awan Clinic, Faisalabad https://orcid.org/0000-0002-5760-912X
Muhammad Haider
Allied Hospital Faisalabad https://orcid.org/0000-0001-6898-2619

Research Article

Keywords: COVID-19, SARS-CoV-2, Ultrasonic Therapy, Conformational States, Phototherapy, Mechanical Stress

Posted Date: April 30th, 2020

DOI: https://doi.org/10.21203/rs.3.rs-25868/v1

Can Mechanical Stress Therapies be used in COVID-19 outbreak?

M. Ali[ϕ]*, M. Haider[χ]

[ϕ] Awan Clinic, Faisalabad, Pakistan

[χ] Allied Hospital Faisalabad, Pakistan

*Corresponding Author: m.alinaeem23@gmail.com; alinaeem023@hotmail.com

Abstract:

Understanding the workings of the novel coronavirus (SARS-CoV-2) is crucial to develop counter therapeutic measures. SARS-CoV-2 gains entry into human cell by binding its receptor Binding Domain (RBD) of Spike protein (S1) to ACE2 receptors. In order to study the effect of mechanical stress on the RBD of SARS-CoV-2, it is modelled as viscoelastic material using Burgers Model. Strain response of RBD under constant stress is analyzed, which gives useful insights into the conformational transitions of RBD at 0K and physiological temperatures. The theoretical underpinning has shown that with increase in the number of stress cycles, the binding affinities of RBD conformational states to ACE2 receptor decrease, decreasing the binding reaction rate between ACE2 receptor and SARS-CoV-2. This analysis gives theoretical evidence that ultrasonic therapy and photo therapy (UV) can be potential candidates to reduce binding reaction rates between ACE2 and SARS-COV-2.

One sentence Summary:

Increasing the no. of stress cycles on RBD of SARS-CoV-2 decreases its binding reaction rate with ACE2 receptor.

SARS-CoV-2 characterized as a member of betacoronavirus genus[1,2], causes COVID-19 disease[3,4]. SARs-CoV-2 uses densely glycosylated spike (S) protein which is a trimeic class I fusion protein [5,6] to enter host cells [7]. S protein exists in metastable prefusion conformation that undergoes a substantial structural rearrangement to fuse viral and host cell membrane [5,6]. This fusion process is triggered when receptor-binding Domain (RBD) of S1 subunit binds with angiotensin-converting enzyme 2 (ACE2) of host cells found in lungs arteries, heart, kidney and intestines[8,9]. Wrapp, et al [7] showed two conformational states of RBD using cryo-electron microscopy. They referred two-conformations as "up" conformation for receptor accessible state and "down" conformation as receptor inaccessible state. The up-conformation is thought to be less stable [10-13]. However, the conformational transitions is critically dependent on temperature [14]. Generally, a protein at cryo-temperatures remains relatively fixed in a particular conformation state and at room temperatures the proteins transitions from one conformation state to the other [14]. The transitions of conformational states can be describe by analogies with non-biological systems such as glass [15-18] and spin glasses [15-17]. The experimental evidence of two-conformational states as presented by Wrapp et al, are two of the many states RBD can transition to depending on the temperature and each conformation state of RBD has different binding Barrier Height H to bind with ACE2. Depending on the barrier Heights, certain conformations of ACE2 have high binding affinity than others, shown at cryo-temperatures by Wrapp, et al [7].

The purpose of this paper is to qualitatively study the conformational transitions of RBD using constant mechanical stress. The logic being to create non-equilibrium state of RBD using mechanical stress and get insights into the transitions to equilibrium states. The first step is to model the RBD, akin to amorphous systems, since amorphous systems share features with

proteins [19]. To serve this purpose, RBD is modelled as a viscoelastic material using 4-element Burger's Model. Excellent reviews of using viscoelasticity for biomaterial modelling have been elegantly exposed, which justifies the RBD of S protein to be viscoelastic in nature. Considerable work is done to describe cellular mechanics using elastic modulus [20]. Furthermore, viscosity measurements are carried out in E-coli plasma membrane [21] and methods are developed to accurately measure energy dissipations using Atomic Force Microscope [22]. However, no data is available for the mechanics of viral protein domain, either experimental or otherwise. Given the constraints, the best one can do is use qualitative analysis using generic solutions of the model. To serve this purpose, the typical strain response of RBD under constant stress, which is analogous to the creep test in materials, is presented. Based on the strain response, the theoretical underpinning of equilibrium energy levels (EELs) of RBD and their corresponding conformational states at 0K temperature is presented, which gives several useful insights into qualitatively characterizing the conformational states at physiological temperatures. Using the premise of EELs and Conformational States, the binding affinity of RBD and ACE2 is discussed in terms of binding Barrier energies, and a region A and region B is characterized where number of high affinity conformational state is high and low, respectively. Based on these regions it is hypothetically reasoned that at a given temperature T, the conformational states of RBD will transition to low binding affinity region B as the number of constant stress cycles increases. Lastly, the use of ultrasonic therapy and phototherapy in transitioning to low affinity region B and reducing the binding rate of RBD and ACE2 is discussed.

Modelling RBD using 4 element Burgers Models

Receptor binding Domain (RBD) of S1 protein is modelled using a 4-element Burgers model [23], which is the combination of Maxwell model and Kelvin-Voight Model connected in series. Burgers model is a constitutive model for linear viscoelasticity, where elasticity and viscosity components are modelled as the linear combinations of springs and viscosity respectively. The configuration of springs with elasticity E_1, E_2 and dashpots with viscosity η_1, η_2 is shown in Figure 1A and the corresponding equation is given by equation 1.

$$\sigma + \left(\frac{\eta_1}{E_2} + \frac{\eta_2}{E_2} + \frac{\eta_2}{E_1}\right)\dot{\sigma} + \frac{\eta_1\eta_2}{E_2E_1}\ddot{\sigma} = \eta_2\dot{\varepsilon} + \frac{\eta_1\eta_2}{E_2}\ddot{\varepsilon} \quad (1)$$

Purely elastic materials do not dissipate energy when load is applied and the material returns to its original configuration, once the load is removed. The viscous component gives the material strain rate dependence in time. Energy is dissipated in the form of heat because of the viscous component, and viscous material loses energy through a loading cycle. At molecular level, elastic components is responsible for the movement of molecules from their equilibrium states, once stress is applied. After stress unloading, the molecules revert back to their original equilibrium states. On the contrary, the viscosity component is responsible for the breaking of sacrificial bonds within the molecules resulting in the energy dissipation, and the deformation of structure is permanent. In this study, the typical strain response under constant stress (creep test) is analyzed and is abstracted for RBD, since proteins share features with amorphous materials [19]. The strain Response under constant stress [23] is given by equation 2.

$$\varepsilon(t) = \sigma_0\left(\frac{1}{E_1} + \frac{1}{E_2}\left(1 - e^{-\frac{tE_2}{\eta_1}}\right) + \frac{t}{\eta_2}\right) \quad (2)$$

where σ_0 is the constant stress. The typical response is shown in Figure 1B, which shows that after a stress loading cycle, a permanent strain ε_{per} stays in the RBD, giving rise to permanent

structure changes in RBD, due to breaking of the sacrificial bonds and dissipation of energy. This is an important insight as after every loading cycle permanent structure change occurs in RBD which results in changes in the conformational states, RBD can attain. The next section uses this insight to develop theoretical underpinning based on the energy levels and corresponding conformational states at these levels.

Theoretical Underpinning

Strain Response of RBD shows that a certain energy e_d is dissipated after a stress loading cycle. This energy dissipation brings RBD to a new energy level, as a results of breakage of sacrificial bonds depending on the viscosity and structure of RBD. Every energy level corresponds to specific conformational states, since the structure at every energy level is different. Furthermore, the number of conformational states of a molecular structure is dependent on the temperature, with low temperatures corresponding to fixed conformational states of the molecular structure. To serve this purpose, it is vital to analyze RBD at absolute zero temperature where conformations are fixed and will only respond to external stimulus.

Equilibrium Energy Levels (EELs) and Conformational States (CS) at 0K Temperature

Consider an arbitrary RBD with total internal energy e_0 at 0K temperature. This internal energy corresponds to a fixed conformational state of RBD. At time $t(L)$ a stress is applied which corresponds to e^* energy added to RBD, increasing the internal energy to Δe_0 where $\Delta e_0 = e_0 + e^*$. This causes RBD to change into a new temporary conformation until e^* is constantly applied. At $t(U)$ RBD is unloaded, hence e^* is removed, RBD jumps to new energy level e_1 after a certain amount of relaxation time t_r . $e_1 < e_0$; as energy e_d is dissipated after unloading. The energy level e_1 corresponds to a new conformational state of RBD. The energy levels e_0 and e_1

are the Equilibrium Energy Levels (EELs), and RBD stays at these levels without external stimulus. The conformational states at EELs are called Equilibrium Conformational states as at 0K temperature conformations are fixed. The transition from e_0 to Δe_0 and from Δe_0 to e_1 are the non-equilibrium energy levels aided by the external stress for e_0 to Δe_0 and energy dissipation as a consequence of external stress from Δe_0 to e_1. The conformational states at non-equilibrium phase are called non-equilibrium conformational states and will naturally be less stable than equilibrium conformational states. Based on this premise, RBD at zero kelvin temperature can have a number of EELs given by e_i where $i = 0,1,2, \dots n$. $i = 0$ is the first natural EEL and n are the total number of EELs. Assuming j number of constant stress cycles are applied to RBD where $j = 1,2,3, \dots . m$ and $j = 1$ is the first loading cycle. e^* amount of energy is added at the time of loading $t(Lj)$., such that at $t(Lj), \Delta e_i = e_i + e^*$. The value of i depends on the number of loading cycle i.e. for $j = 1; i = 0$ and for $j + 1; i + 1$. Furthermore, assume at the time of unloading $t(Uj)$, e^* is instantaneously removed such that at $t(Uj); e_i = \Delta e_i - e^*$. The total loading time t_i is given by the difference between the time of unloading $t(Uj)$ and time of loading $t(Lj)$ i.e. $t_i = t(Uj) - t(Lj)$. As a first linear approximation, assume after every loading cycle, e_d amount of energy is dissipated linearly with time, which is a crude first approximation, as energy dissipation depends on the viscosity and structure, which may change after each loading cycle, Nonetheless, this approximation is very insightful in the broader scheme. The relaxation time t_r is the difference between the time where $\frac{d}{dt} e_d = 0$ from the time of unloading (Uj) . After relaxation time, RBD jumps to a new EEL and correspondingly a new conformational state. The new EEL after each loading cycle can be given by $e_{i+1} = e_i - e_d$. Assuming, as a first approximation $\frac{d}{dt} e_d$ is a linear decreasing function with

time t and is same for every loading cycle, the EELs of RBD of S1 protein at 0K Temperature is shown in Figure 2.

As mentioned above, each EEL e_i of RBD has a fixed equilibrium CS given by C_i. The transition period from one EEL to the other corresponds to non-equilibrium conformational states given by $\overline{C_\iota}$. Both equilibrium C_i and non-equilibrium $\overline{C_\iota}$ prefusion conformational states of RBD of S1 protein have specific binding Energy Barrier to bind with ACE2 receptor, which corresponds to specific binding affinities of different CS to ACE2 receptor. Let the binding Energy Barrier for equilibrium CS be H_i and non-equilibrium CS be $\overline{H_\iota}$. The typical binding reaction between equilibrium and non-equilibrium CS of RBD of S1 protein and ACE2 receptor is given by equation 3 and 4 respectively

$$C_i(RBD) + ACE2 \overset{H_i}{\rightarrow} C_i(RBD)ACE2 \tag{3}$$

$$\overline{C_\iota}(RBD) + ACE2 \overset{\overline{H_\iota}}{\rightarrow} C_i(RBD)ACE2 \tag{4}$$

RBD conformational states with low H_i and $\overline{H_\iota}$ will generally have high binding affinity with ACE2 receptor, making certain conformations to fuse easily with ACE2 than others. Likewise certain CS will have zero affinity to bind with ACE2, as energy barrier of reaction are large to overcome. Wrapp. Et al have shown a CS denoted by “down” CS at cryo-temperatures which have zero affinity to bind with ACE2 receptor [7].

The next step is to establish a region where CS have high affinity to fuse with ACE2 receptor. For any biological reaction, the molecular structure of reactants is of paramount importance, as certain molecular bonds are broken and new bonds are made during the chemical reaction. So, for RBD to bind with ACE2, the structural integrity of RBD will have significant impact on the

binding affinity with ACE2. It has been shown, after every load cycle, sacrificial bonds are broken, deforming the structure of RBD. The exact sacrificial bond breakage during each cycle requires further study, however, it is fairly straightforward to establish that after enough load cycles, large number of bonds will be broken in RBD, making it structurally unfavorable to bind with ACE2. Furthermore, low energy levels generally have high stabilities and have to overcome large energy Barriers. Using these premises, it can be hypothesized that as the number of load cycles increase, the binding affinities of CS of RBD with ACE2 will decrease, because of structural deterioration and high binding energy barriers. An arbitrary RBD of S1 protein of SARS-CoV-2 shows high binding affinity with ACE2 receptor because of its genetic makeup. So using stress loading cycles, one can deform molecular structure of RBD, making it unfavorable to bind with ACE2. No information is available yet about the sacrificial bonds which will break upon loading. The best one can do is establish a region starting from its natural state where it has high binding affinity. As the number of load cycles increase, the binding affinity of both C_i and $\overline{C_i}$ will tend to decrease for the reasons mentioned earlier. Consider an RBD in its natural state with EEL e_0, which has high binding affinity to react with ACE2. After a number of load cycles, the structure however deformed may still have the CS capable to bind with ACE2 with high affinity. Let this region be denoted by Region A (Figure 2). As one move away from Region A towards Region B (Figure 2), the binding affinities of CS both C_i and $\overline{C_i}$ will decrease, because of structural deformations and high energy barriers. After a certain number of load cycle, the structure will become unfavorable for binding with ACE2.

EELs and CS at Physiological Temperatures

Using the analysis at 0K temperature, one can get useful insights at the physiological temperatures. At physiological temperatures, proteins undergo equilibrium fluctuations, causing

it to move from one CS to another at nearly isoenergies. Consider an arbitrary RBD in its natural state at physiological temperature T. At this temperature CS of RBD transition dynamically from one conformational state to another. The energy levels of RBD fluctuates as a result of dynamic conformational transitions. Consider an energy level e_0 which is the central value around which the energy level fluctuations deviates. This energy level e_0 is the EEL. Assuming in its natural energy state e_0 at physiological temperature T, RBD has $C_{0,x}$ conformational states, where 0 represents energy level e_0 and $x = 1,2,3, \dots y$, with y are the total number of CS. The total number of energy level deviations from EEL e_0 will be y, each deviation resulting from a specific conformational state. The absolute deviation D_x of the fluctuations is given by $D_x = |e_{0,x} - e_0|$ where $e_{0,x}$ is the energy level fluctuations specific to conformational states. Constant stress is applied, supplying e^* amount of energy to RBD. The energy increases to Δe_0 where $\Delta e_0 = e_0 + e^*$, it has been assumed $\Delta e_0 \gg D_x$. Once the stress is unloaded, the energy level falls after relaxation time t_r to a new energy level e_1, around which the new conformational states with specific energies deviate. During loading and relaxation time, RBD undergoes non-equilibrium CS given by $\overline{C_{0,x}}$. Based on the premises at 0K temperature, EELs at physiological temperatures are given by e_i, where $i = 0,1,2, \dots$ n and n are the total number of EELs around which the energy levels deviates. The equilibrium CS at a given EEL e_i are given by $C_{i,x}$, where i is the EEL and x represents CS fluctuating at that energy level and $x = 1,2,3, \dots y$. The total number of CS fluctuations at e_i are y. The absolute deviations at EEL e_i are given by $D_{i,x} = |e_{i,x} - e_i|$ Likewise, the non-equilibrium CS are given by $\overline{C_{i,x}}$, which occurs during the transition from one EEL to the other.

As established for 0K temperature, each CS (equilibrium and non-equilibrium) has a specific binding energy barrier to ACE2 receptor given by equation 3 and 4. Likewise, at physiological

temperatures, each CS ($C_{i,x}$ and $\overline{C_{\iota,x}}$) has specific binding energy barrier ($H_{i,x}$ and $\overline{H_{\iota,x}}$). Depending on the values of $H_{i,x}$ and $\overline{H_{\iota,x}}$, the binding affinities of $C_{i,x}$ and $\overline{C_{\iota,x}}$ with ACE2 receptors will vary. High $H_{i,x}$ and $\overline{H_{\iota,x}}$ corresponds to low binding affinities with ACE2 receptor. As established for 0K temperature, it can be hypothesized that as the number of load cycles increase, the binding affinities of CS will decrease, and energy levels of RBD will transition from high affinity Region A to low affinity Region B (Figure 2).

Zero Affinity and greater than Zero Affinity CS

Consider an arbitrary RBD at physiological temperature with total conformational states (both equilibrium and non-equilibrium) at all EELs to be C_{tot}. Total conformational states is the sum of CS with zero affinity C_{zero} to bind with ACE2 receptor and CS with greater than zero affinity C_{aff} to bind with ACE2 receptor. i.e. $C_{tot} = C_{zero} + C_{aff}$. Consider a sample of Z number of RBD of SARS-COV-2 at physiological temperature. The total number of CS of Z number of RBD is given by $C_{tot} = ZC_{zero} + ZC_{aff}$. The binding reaction rate R of the sample Z with ACE2 receptor depends on the number of ZC_{aff}. As the number of ZC_{aff} decreases, the reaction rate of RBD and ACE2 receptor will decrease, since the number of CS have binding affinity greater than zero in the sample are less. It has been hypothetically established earlier, that as the number of stress cycles increase, CS transitions towards low affinity states and after a certain number of cycles, affinity becomes zero. In principle, if the number of stress cycles on sample Z is increased, the reaction rate R between RBD of SARS-CoV-2 and ACE2 receptors will decrease. It should be mentioned that this hypothesis stands for all type of viral structures including SARS-CoV-1 as well as other protein domains. The difference among species arise because of different CS and different RBD mechanics.

Therapeutic Options at Physiological Temperatures

The viscoelastic nature of RBD of SARS-CoV-2 makes ultrasound therapy suitable to apply mechanical energy to RBD. Viscoelastic materials coverts mechanical energy from vibrations of ultrasound energy to thermal energy. Sacrificial bonds in the materials are broken as a result, deforming their structure. Ultrasonic therapy is therefore a viable therapeutic option for mechanically loading the RBD of SARS-CoV-2, and reducing the binding reaction rate R between RBD and ACE2 receptor. However, the analysis of conformations so far is done using constant stress and mechanical stressing by ultrasound waves are oscillatory, which requires dynamic mechanical analysis, but the principles of conformational transitions and binding affinities at constant stress holds.

Phototherapy using ultraviolet (UV) electromagnetic waves can be another viable option. Considerable research has already been elegantly exposed on the effect of UV on SARS-CoV-1. Duan et al. has shown the destruction of infectivity of SARS coronavirus strain CoV-P9 after 60 minutes of irradiation [24]. Kariwa et al. has also shown reduction of infectivity of SARS-COV under UV irradiation [25]. UV irradiation uses energy in the form of photons to break sacrificial bonds in RBD, reducing number of CS with binding affinities greater than zero and as a consequence reducing binding reaction rate between ACE2 and SARS-CoV-2. However, both these therapeutic options require further progresses both experimentally and theoretically. Nonetheless, these options are worth exploring as potential candidates for reducing the reaction rate between SARS-CoV-2 and ACE2 receptor.

Conclusion

To develop useful therapeutic countermeasures against SARS-CoV-2, which has caused global pandemic, understanding the workings of the virus is of utmost importance. Understanding the conformational transitions of Receptor Binding Domain of SARS-CoV-2 is vital to know and alter the binding affinities and reaction rate between SARS-CoV-2 and ACE2 receptor. Furthermore, therapeutic options can be optimized based on the understanding of conformational states of RBD. Based on the knowledge presented here, Ultrasound and photo therapies have the potential to decrease the binding reaction rate of SARS-CoV-2 and ACE receptor. This paper serves as the first step and requires further experimental and theoretical progress. The ideas in this paper will be very useful in developing medical countermeasures against the virus including vaccines.

References:

1. R. Lu, X. Zhao, J. Li, P. Niu, B. Yang, H. Wu, W. Wang, H. Song, B. Huang, N. Zhu, Y. Bi, X. Ma, F. Zhan, L. Wang, T. Hu, H. Zhou, Z. Hu, W. Zhou, L. Zhao, J. Chen, Y. Meng, J. Wang, Y. Lin, J. Yuan, Z. Xie, J. Ma, W. J. Liu, D. Wang, W. Xu, E. C. Holmes, G. F. Gao, G. Wu, W. Chen, W. Shi, W. Tan, Genomic characterisation and epidemiology of 2019 novel coronavirus: Implications for virus origins and receptor binding. *Lancet* S0140-6736(20)30251-8 (2020). doi:10.1016/S0140-6736(20)30251-8pmid:32007145
2. F. Wu, S. Zhao, B. Yu, Y.-M. Chen, W. Wang, Z.-G. Song, Y. Hu, Z.-W. Tao, J.-H. Tian, Y.-Y. Pei, M.-L. Yuan, Y.-L. Zhang, F.-H. Dai, Y. Liu, Q.-M. Wang, J.-J. Zheng, L. Xu, E. C. Holmes, Y.-Z. Zhang. A new coronavirus associated with human respiratory disease in China. *Nature* (2020). doi:10.1038/s41586-020-2008-3pmid:32015508
3. J. F. Chan, S. Yuan, K.-H. Kok, K. K.-W. To, H. Chu, J. Yang, F. Xing, J. Liu, C. C.-Y. Yip, R. W.-S. Poon, H.-W. Tsoi, S. K.-F. Lo, K.-H. Chan, V. K.-M. Poon, W.-M. Chan, J. D. Ip, J.-P. Cai, V. C.-C. Cheng, H. Chen, C. K.-M. Hui, K.-Y. Yuen, A familial cluster of pneumonia associated with the 2019 novel coronavirus indicating person-to-person transmission: A study of a family cluster. *Lancet* **395**, 514–523 (2020). doi:10.1016/S0140-6736(20)30154-9pmid:31986261
4. C. Huang, Y. Wang, X. Li, L. Ren, J. Zhao, Y. Hu, L. Zhang, G. Fan, J. Xu, X. Gu, Z. Cheng, T. Yu, J. Xia, Y. Wei, W. Wu, X. Xie, W. Yin, H. Li, M. Liu, Y. Xiao, H. Gao, L. Guo, J. Xie, G. Wang, R. Jiang, Z. Gao, Q. Jin, J. Wang, B. Cao, Clinical features of patients infected with 2019 novel coronavirus in Wuhan, China. *Lancet* **395**, 497–506 (2020). doi:10.1016/S0140-6736(20)30183-5pmid:31986264

5. F. Li, Structure, Function, and Evolution of Coronavirus Spike Proteins. *Annu. Rev. Virol*. **3**, 237–261 (2016). doi:10.1146/annurev-virology-110615-042301pmid:27578435

6. B. J. Bosch, R. van der Zee, C. A. de Haan, P. J. Rottier, The coronavirus spike protein is a class I virus fusion protein: Structural and functional characterization of the fusion core complex. *J. Virol*. **77**, 8801–8811 (2003). doi:10.1128/JVI.77.16.8801-8811.2003pmid:12885899

7. Wrapp, D., Wang, N., Corbett, K.S., Goldsmith, J.A., Hsieh, C.L., Abiona, O., Graham, B.S., Mclellan, J.S. Cryo-EM structure of the 2019-nCoV spike in the prefusion conformation. Science. 367(6483) 1260-1263 (2020). Doi: 10.1126/science.abb2507

8. Hamming, I., Timens, W., Bulthuis, M.L., Lely, A.T., Navis, G., van Goor, H. Tissue distribution of ACE2 protein, the functional receptor for SARS coronavirus. A first step in understanding SARS pathogenesis. *The Journal of Pathology*. **203** (2): 631–7. (June 2004) doi:10.1002/path.1570

9. Donoghue, M., Hsieh, F., Baronas, E., Godbout, K., Gosselin, M., Stagliano, N., Donovan, M., Woolf, B., Robison, K., Jeyaseelan, R., Breitbart, R.E., & Acton S. A Novel Angiotensin-Converting Enzyme–Related Carboxypeptidase (ACE2) Converts Angiotensin I to Angiotensin 1-9. *Circulation Research*. **87** (5): e1–e9. (1 Sep 2000) doi:10.1161/01.RES.87.5.e1

10. M. Gui, W. Song, H. Zhou, J. Xu, S. Chen, Y. Xiang, X. Wang, Cryo-electron microscopy structures of the SARS-CoV spike glycoprotein reveal a prerequisite conformational state for receptor binding. *Cell Res*. **27**, 119–129 (2017). doi:10.1038/cr.2016.152pmid:28008928

11. J. Pallesen, N. Wang, K. S. Corbett, D. Wrapp, R. N. Kirchdoerfer, H. L. Turner, C. A. Cottrell, M. M. Becker, L. Wang, W. Shi, W.-P. Kong, E. L. Andres, A. N. Kettenbach, M. R. Denison, J. D. Chappell, B. S. Graham, A. B. Ward, J. S. McLellan, Immunogenicity and structures of a rationally designed prefusion MERS-CoV spike antigen. *Proc. Natl. Acad. Sci. U.S.A.* **114**, E7348–E7357 (2017). doi:10.1073/pnas.1707304114pmid:28807998

12. A. C. Walls, X. Xiong, Y.-J. Park, M. A. Tortorici, J. Snijder, J. Quispe, E. Cameroni, R. Gopal, M. Dai, A. Lanzavecchia, M. Zambon, F. A. Rey, D. Corti, D. Veesler, Unexpected receptor functional mimicry elucidates activation of coronavirus fusion. *Cell* **176**, 1026–1039.e15 (2019). doi:10.1016/j.cell.2018.12.028pmid:30712865

13. Y. Yuan, D. Cao, Y. Zhang, J. Ma, J. Qi, Q. Wang, G. Lu, Y. Wu, J. Yan, Y. Shi, X. Zhang, G. F. Gao, Cryo-EM structures of MERS-CoV and SARS-CoV spike glycoproteins reveal the dynamic receptor binding domains. *Nat. Commun.* **8**, 15092 (2017). doi:10.1038/ncomms15092pmid:28393837

14. Frauenfeld, H., Sligar, S.G., Wolynes, P.G. The energy landscapes and motions of proteins. *Science*. **254**(5038), 1598-603 (1991). Doi: 10.1126/science.1749933

15. R. Zallen, The Physics of Amorphous Solids (Wiley, New York, 1983)

16. W. A. Phillips, Ed., Amorphous Solids (Springer, Berlin, 1981);

17. Stillinger, F.H., & Weber, T. Packing Structures and Transitions in Liquids and Solids. *Science* **225**(4664), 983-989 (1984). DOI: 10.1126/science.225.4666.983

18. Jackle, J. Models of the glass transition. *Rep. Prog. Phys.* **49**, 171 (1986). https://doi.org/10.1088/0034-4885/49/2/002

19. I. E. T. Iben et al., Glassy behavior of a protein. *Phys. Rev. Lett*. **62**, 1916 (1989). https://doi.org/10.1103/PhysRevLett.62.1916

20. Guz, N., Dokukin, M., Kalaparthi, V., Sokolov, I. If cell mechanics can be described by elastic modulus: study of different models and probes used in indentation experiments. *Biophys J*.**107**(3):564–575 (2014). doi:10.1016/j.bpj.2014.06.033

21. Mika, J.T., Thompson, A.J., Dent, M.R., et al. Measuring the Viscosity of the Escherichia coli Plasma Membrane Using Molecular Rotors. *Biophys J.* **111**(7):1528–1540 (2016). doi:10.1016/j.bpj.2016.08.020

22. Biswas, S., Leitao, S., Theillaud, Q., Erickson, B.W., Fantner, G.E. Reducing uncertainties in energy dissipation measurements in atomic force spectroscopy of molecular networks and cell-adhesion studies. *Sci Rep.* **8**(1) 9390 (2018). doi:10.1038/s41598-018-26979-0

23. Mainardi, F. & Spada, G. Creep, Relaxation and Viscosity Properties for Basic Fractional Models in Rheology. *The European Physical Journal, Special Topics*, **193** (2011) 133–160. https://arxiv.org/pdf/1110.3400.pdf

24. Duan, S.M., Zhao, X.S., Wen, R.F., et al. Stability of SARS coronavirus in human specimens and environment and its sensitivity to heating and UV irradiation. *Biomed Environ Sci*. **16**(3):246–255 (2003). PMID: 14631830

25. Kariwa, H., Fujii, N., Takashima, I. Inactivation of SARS coronavirus by means of povidone-iodine, physical conditions, and chemical reagents. *Jpn J Vet Res*. **52**(3):105–112 (2004). PMID: 15631008

Acknowledgments:

The authors will like to acknowledge the support of Dr. Naeem Akhtar, Jia Naeem, Asma, Shabina and Dr. Zunaira.

Competing interests: The authors declare no competing interests.

Author Contributions:

Muhammad Ali: First Author

Muhammad Haider: Insights into RBD and ACE2 reactions and helped with manuscript preparation.

List of Supplementary Material:

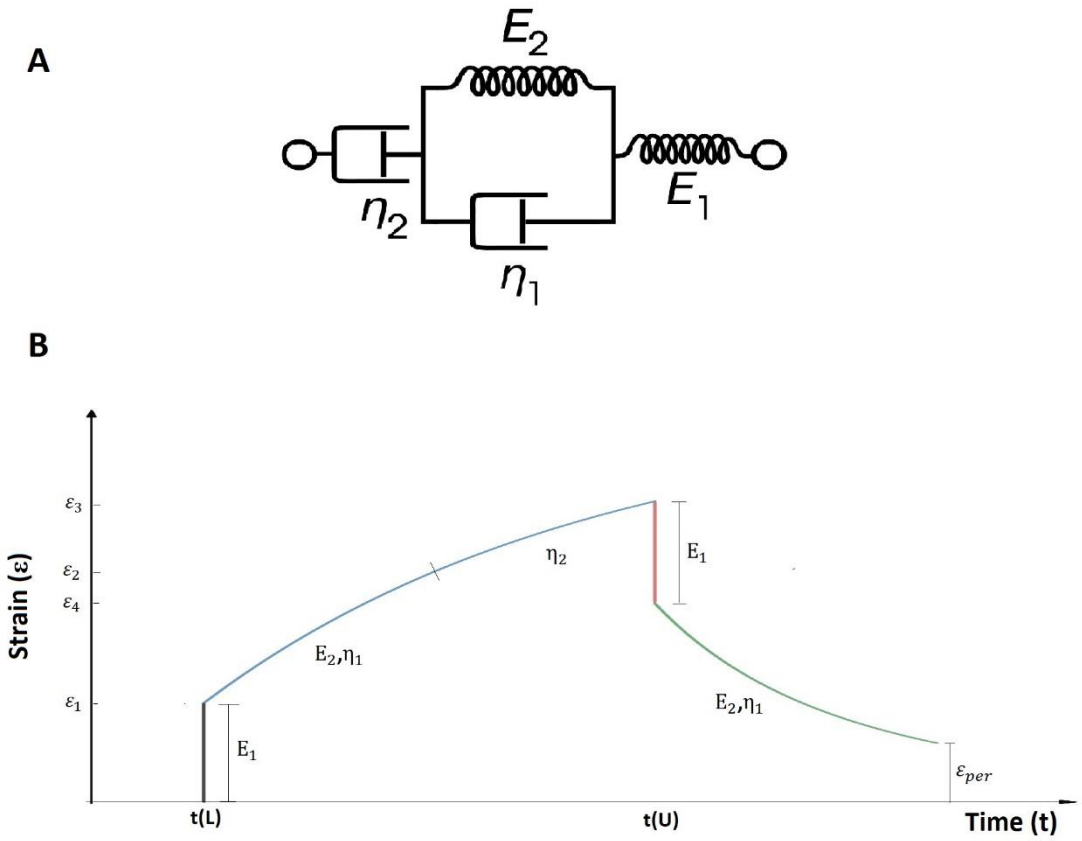

Figure 1. Configuration and Strain Response under constant stress.

(A) Configuration of springs with elasticities (E_1,E_2) and Dashpots with viscosities (η_1, η_2) in 4-element Burgers Models.

(B) Strain Response under constant stress cycle. Stress is applied at $t(L)$, which corresponds to instantaneous strain ε_1 due to elasticity E_1 of spring. Followed by the increase in strain to ε_2 due to elasticity and viscosity E_2 and η_1 respectively. The strain continue to increase until ε_3 because of viscosity of dashpot η_2. At $t(L)$, the stress is unloaded which corresponds to a sudden decrease in strain to ε_4 due to elasticity E_1 of spring. The strain continue to decrease at a decreasing strain rate due to elasticity $E_2$and viscosity $\eta_1$of spring and dashpot respectively. Permanent strain in the system remain equal to ε_{per} after one stress cycle which is due to the viscosity η_2 of dashpot. The system in this case RBD has permanent structural changes after the loading cycle.

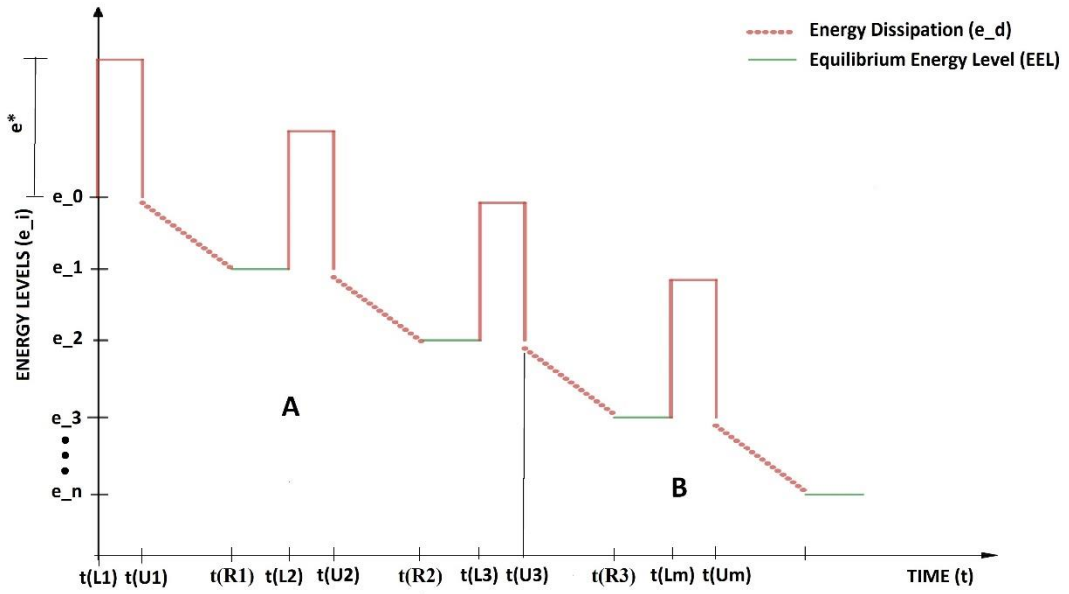

Figure 2. Transition of EELs and CS of RBD of S1 protein at 0K Temperature as a result of Stress Cycles. The energy dissipation e_d is approximated to be linear decreasing function with time i.e. $\frac{de_d}{dt}$ and remains same at each loading cycle. The total loading time t_l is given by $t(Uj) - t(Lj)$ where $j = 1,2,3, \ldots . m$. The relaxation time t_r is given by $t_r = t(Rj) - t(U[j-1])$. Each e_i(green line) corresponds to a specific equilibrium conformational State C_i where $i = 0,1,2,3, \ldots . n$. The Transition between EELs corresponds to non-equilibrium conformational states $\overline{C_i}$. C_i is more stable than $\overline{C_i}$. Each C_i and $\overline{C_i}$ has different binding Barrier Energies and binding affinities with ACE2 receptor. Region A has hypothesized to have more C_i and $\overline{C_i}$ with high binding affinities to ACE2 receptor than Region B.

Figures

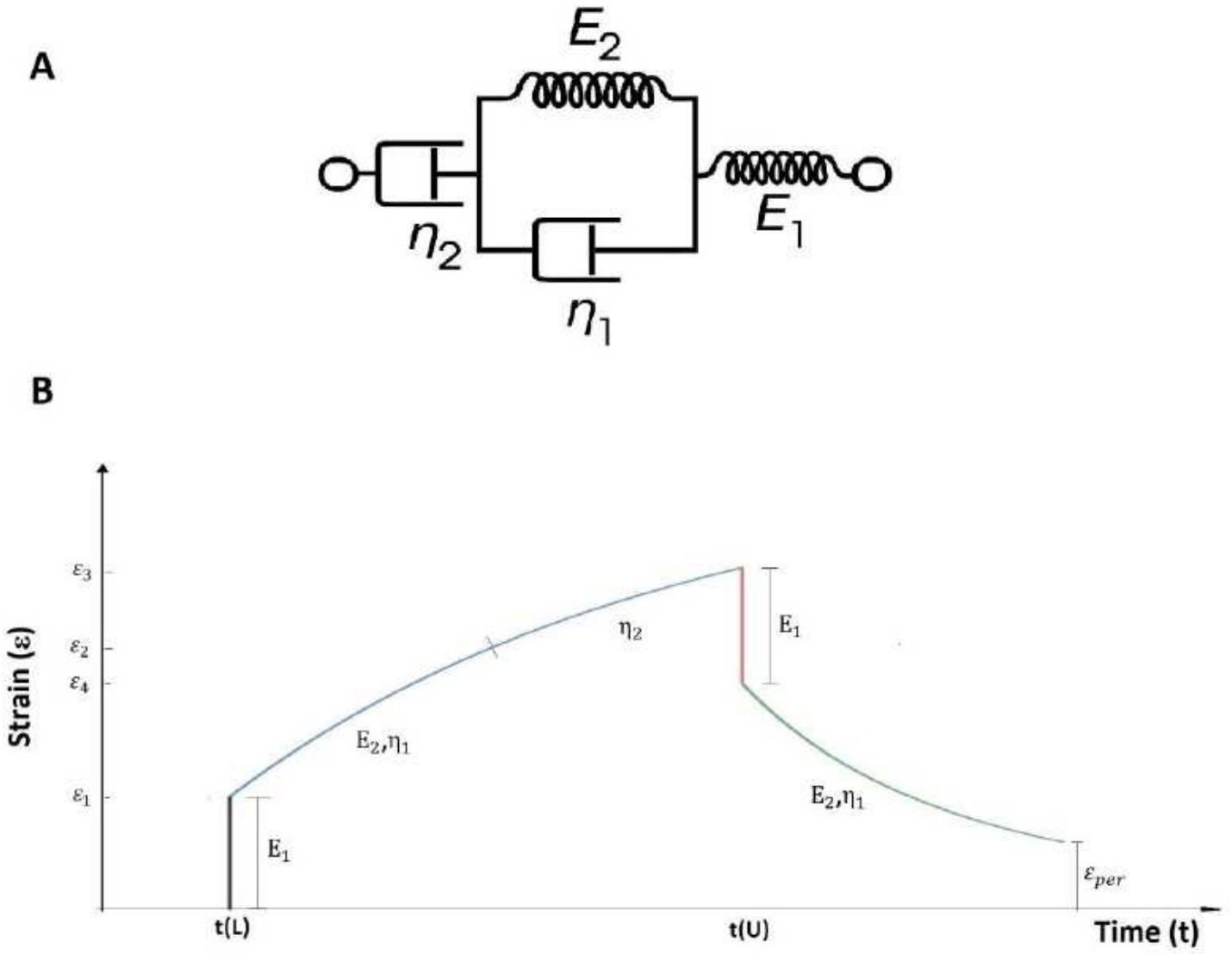

Figure 1

Configuration and Strain Response under constant stress. (A) Configuration of springs with elasticities (□1,□2) and Dashpots with viscosities (□1,□2) in 4-element Burgers Models. (B) Strain Response under constant stress cycle. Stress is applied at □(□), which corresponds to instantaneous strain □1 due to elasticity □1 of spring. Followed by the increase in strain to □2 due to elasticity and viscosity □2 and □1 respectively. The strain continue to increase until □3 because of viscosity of dashpot □2. At □(□), the stress is unloaded which corresponds to a sudden decrease in strain to □4 due to elasticity □1 of spring. The strain continue to decrease at a decreasing strain rate due to elasticity □2and viscosity □1of spring and dashpot respectively. Permanent strain in the system remain equal to □□□□ after one stress cycle which is due to the viscosity □2 of dashpot. The system in this case RBD has permanent structural changes after the loading cycle.

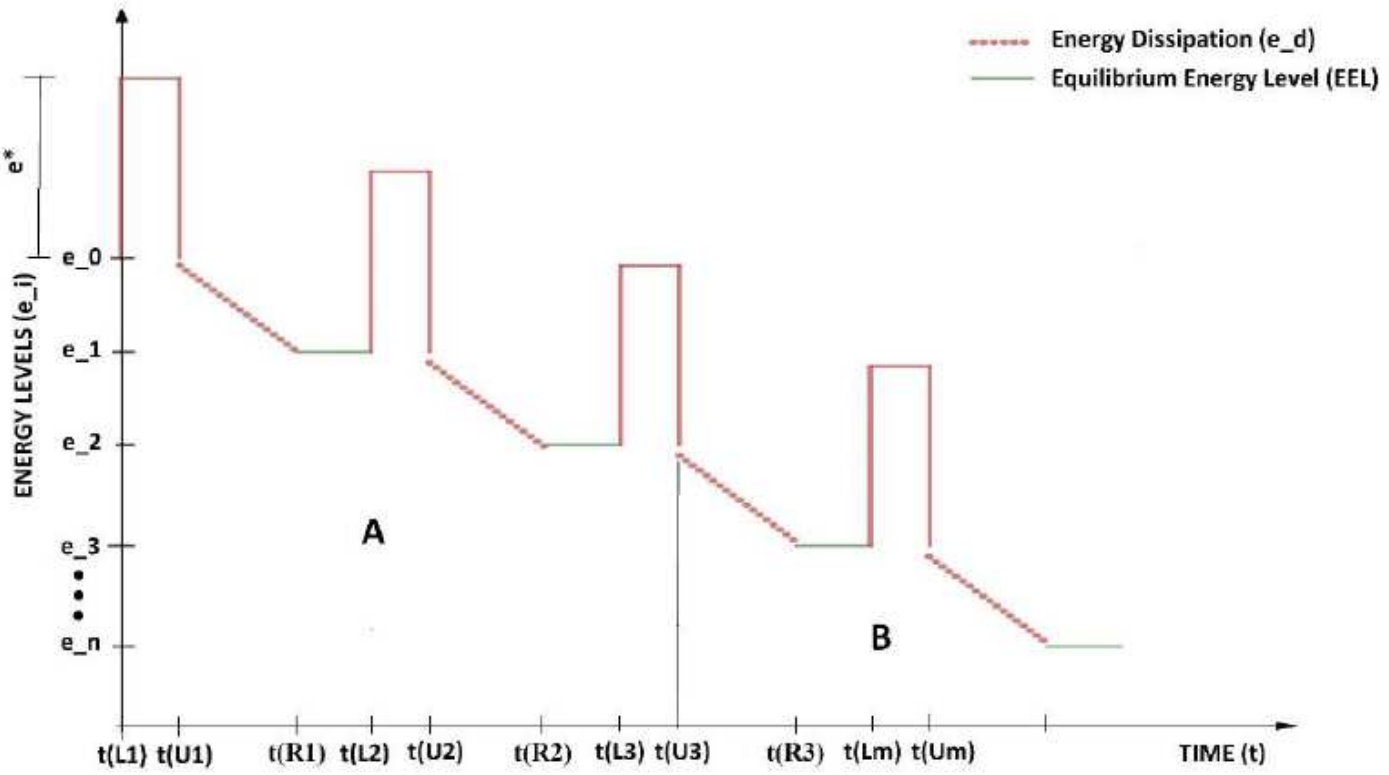

Figure 2

Transition of EELs and CS of RBD of S1 protein at 0K Temperature as a result of Stress Cycles. The energy dissipation □□ is approximated to be linear decreasing function with time i.e. □□□□□ andremains same at each loading cycle. The total loading time □□ is given by □(□□)−□(□□) where □=1,2,3,….□. The relaxation time □□ is given by □□=□(□□)−□(□[□−1]). Each □□(green line) corresponds to a specific equilibrium conformational State □□ where □=0,1,2,3,….□. The Transition between EELs corresponds to non-equilibrium conformational states □□□□□. □□ is more stable than □□□. Each □□ and □□□ hasdifferent binding Barrier Energies and binding affinities with ACE2 receptor. Region A has hypothesized to have more □□ and □□□ with high binding affinities to ACE2 receptor than Region B.